Yb$_7$Ni$_4$InGe$_{12}$: A Quaternary Compound Having Mixed Valent Yb atoms Grown from Indium Flux

Udumula Subbarao[1], Rajkumar Jana[1], Maria Chondroudi[2], Mahalingam Balasubrmanian[3], Mercouri G. Kanatzidis[2,4], Sebastian C. Peter[1]*

[1]New Chemistry Unit, Jawaharlal Nehru Centre for Advanced Scientific Research, Jakkur, Bangalore, 560064, India

[2]Materials Science Division, Argonne National Laboratory, Argonne, IL 60439

[3]Advanced Photon Source, Argonne National Laboratory, Argonne, IL 60439

[4]Department of Chemistry, Northwestern University, 2145 N. Sheridan Road, Evanston, IL 60208-3113, USA.

Abstract

The new intermetallic compound Yb$_7$Ni$_4$InGe$_{12}$ was obtained as large silver needle shaped single crystals from reactive indium flux. Single crystal X-ray diffraction suggest that Yb$_7$Ni$_4$InGe$_{12}$ crystallizes in the Yb$_7$Co$_4$InGe$_{12}$ structure type, tetragonal space group $P4/m$ and lattice constants are $a = b = 10.291(2)$ Å and $c = 4.1460(8)$ Å. The crystal structure of Yb$_7$Ni$_4$InGe$_{12}$ consists of columnar units of three different types of channels filled with the Yb atoms. The crystal structure of Yb$_7$Ni$_4$InGe$_{12}$ is closely related to Yb$_5$Ni$_4$Ge$_{10}$. The effective magnetic moment obtained from the magnetic susceptibility measurements in the temperature range 200-390 is 3.66 μ_B/Yb suggest mixed/intermediate valence behavior of ytterbium atoms. X-ray absorption near edge spectroscopy (XANES) confirms that Yb$_7$Ni$_4$InGe$_{12}$ exhibits mixed valence.

* Corresponding author. Phone: 080-22082998, Fax: 080-22082627
sebastiancp@jncasr.ac.in (S. C. Peter); m-kanatzidis@northwestern.edu (M. G. Kanatzidis)

Dalton Transactions Accepted Manuscript

1. Introduction

In general, intermetallic compounds are synthesized by conventional techniques such as arc melting and high frequency induction furnace heating. However, europium and ytterbium based compounds are difficult to synthesize by these methods due to their low boiling points. This limitation overall resulted in fewer number of europium and ytterbium compounds studied in the past compared to other rare earth based compounds. However, recently, the use of metal flux has emerged as an excellent tool to produce many novel ternary and quaternary intermetallic phases.[1-27] Among the metal fluxes, very recently, indium has been exploited for the crystal growth of quaternary compounds.[28-36] One of the interesting features of the metal flux synthesis method is in the reduction of melting point and vapor pressure of the starting materials, which resulted in the formation of new compounds. A good review about the concept and use of metal flux technique for the formation of new compounds was reported by Kanatzidis and co-workers.[37]

Among the rare earths, as known and detailed by us before, the Yb containing compounds have particular scientific interest due to its ability to exhibit two energetically similar electronic configurations: the magnetic Yb^{3+} ($4f^{13}$) and the nonmagnetic Yb^{2+} ($4f^{14}$) one.[11] In this case, the roles of the 4f electron and 4f hole can be interchanged and Yb based compounds often crystallize in new structure types.[38-40] Due to these reasons, Yb based compounds exhibit various peculiar properties such as intermediate valence, heavy fermions, Kondo behavior, unusual magnetism[41-45] and superconductor at low temperature.[46, 47] These properties are generally believed to arise from the strong hybridization (interaction) between the localized 4f electrons and the delocalized s, p, d conduction electrons.[48-50]

In the last several years, we have focused our research to the intermetallic chemistry of Yb based compounds[51-55] and sought deeper understanding of the ability of Yb to adopt different structure types. During the systematic studies on the compounds in the Yb-Ni-Ge family, a new quaternary compound $Yb_7Ni_4InGe_{12}$ was obtained from the reaction run in In flux. There are several compounds reported in the Yb-Ni-Ge family; $YbNiGe$,[56, 57] $YbNi_{0.25}Ge_{1.25}$,[56] $YbNiGe_2$,[28] $YbNiGe_3$,[56] $YbNi_2Ge_2$,[56, 58] $YbNi_5Ge_3$,[56] $YbNi_{4.4}Ge_{0.6}$,[56] Yb_2NiGe_6,[56, 59] $Yb_2Ni_{15.1}Ge_{1.9}$,[56] $Yb_3Ni_{11}Ge_4$[56] and $Yb_5Ni_4Ge_{10}$.[60] So far only a few quaternary polyindides with an impressive set of diverse structures and compositions have been synthesized using In as active solvent. Chondroudi *et al.* reported the quaternary compounds $RE_7Co_4InGe_{12}$ (RE = Dy, Ho, Yb),[36] which contains mixed-valent Yb and trivalent Dy and Ho. In this family, $Dy_4Ni_2InGe_4$, $Ho_4Ni_2InGe_4$ and $Er_4Ni_2InGe_4$ show antiferromagnetic transitions at low temperature. On other hand, $Tm_4Ni_2InGe_4$ has no magnetic ordering down to the lowest temperature attainable. $Yb_3AuGe_2In_3$ is another example having mixed valent Yb grown from In flux which crystallizes as an ordered variant of the YbAuIn structure.[61] Apart from these interesting compounds several quaternary indides worth mentioning are $REMn_2In_xZn_{20-x}$ (RE = Ce-Sm, Gd, Dy, Er, Yb),[62] $REMn_6InSn_5$ (RE = Ho, Tm),[63] $Ce_2NiPdIn$,[64] $CeNiX_3In$ (X =Al, Ga),[65] $RE_7Ni_{5-x}Ge_{3+x}In_6$ (RE = La, ND, Sm)[66] and $CeCuAgIn$.[67]

In this paper, we report the synthesis of a new quaternary compound $Yb_7Ni_4InGe_{12}$. $Yb_7Ni_4InGe_{12}$ is isostructural to the $RE_7Co_4InGe_{12}$ family, which is closely related to the structure of $Yb_5Ni_4Ge_{10}$.[60] Magnetic susceptibility measurements were performed on the selected single crystals of $Yb_7Ni_4InGe_{12}$ suggests mixed valent behavior of Yb atoms, which was confirmed by X-ray absorption near edge spectroscopy (XANES) measurement.

3

2. Experimental Section

2.1 Reagents: The following reagents were used as purchased from Alfa Aesar without further purification: Yb (in the form of metal pieces cut from metal chunk, 99.99%), Ni (powder, 99.99%), Ge (pieces, 99.99%) and In (shots, 99.99%).

2.2 Synthesis of $Yb_7Ni_4InGe_{12}$

The synthesis of $Yb_7Ni_4InGe_{12}$ was performed by combining ytterbium metal (0.4 g), nickel (0.07 g), germanium (0.2 g) and indium (2.32 g) in an alumina crucible. The crucible was placed in a 13 mm diameter fused silica tube, under an inert (argon) atmosphere inside a glove box, which was flame sealed under a vacuum of 10^{-5} torr to prevent oxidation during heating. The reactants were then heated to 1000 °C over 10 h, maintained at that temperature for 5 h to allow proper homogenization, then cooled to 850 °C in 2 h and kept at this temperature for 48 h. Finally, the sample was allowed to cool down to 30 °C over 48 h. The reaction product was isolated from the excess indium flux by heating at 400 °C and subsequently centrifuging through a coarse frit. Any unreacted flux was removed by immersion and sonication in glacial acetic acid for 24 h. The final crystalline product was rinsed with water and dried with acetone. This method produced the target compound $Yb_7Ni_4InGe_{12}$ with ca. 90% purity and relatively in a high yield (ca. 60%) on the basis of the initial amount of Yb metal used in the reaction. Suitable needle shaped crystals of $Yb_7Ni_4InGe_{12}$ were carefully selected for the single crystal XRD data collection and magnetic measurements.

2.3 Single-Crystal X-ray Diffraction

Suitable single crystal of $Yb_7Ni_4InGe_{12}$ was mounted on a thin glass fiber with commercially available super glue. X-ray single crystal structural data was collected on a

Bruker Smart CCD diffractometer equipped with a normal focus, 2.4 kW sealed tube X-ray source with graphite monochromatic Mo-Kα radiation ($\lambda = 0.71073$ Å) operating at 50 kV and 30 mA, with ω scan mode. The software programme SAINT[68] was used for integration of diffraction profiles and absorption correction were made with SADABS programme.[69] The structure was solved by SHELXS 97 and refined by a full matrix least-squares method using SHELXL.

2.4 Structure refinement

X-ray single crystal data of $Yb_7Ni_4InGe_{12}$ showed that the compound crystallizes in the primitive tetragonal lattice ($P4/m$) within the $Yb_7Co_4InGe_{12}$ type structure and lattice constants are $a = b = 10.291(2)$ Å and $c = 4.1460(8)$ Å. The atomic parameters of the $Yb_7Co_4InGe_{12}$ structure were taken as starting values and the crystal structure of $Yb_7Ni_4InGe_{12}$ was refined using Shelxl-97 (full-matrix least-squares on F^2)[70] with anisotropic atomic displacement parameters for all the atoms. As a check for the correct composition, the occupancy parameters were refined in a separate series of least-squares cycles. This refinement resulted in eight atomic sites fully occupied within two standard uncertainties. All bond lengths are within the acceptable range compared to the expected values.[59, 71, 72] The overall stoichiometry obtained from the refinement is $Yb_7Ni_4InGe_{12}$.

The data collection and structure refinement details for $Yb_7Ni_4InGe_{12}$ are listed in Table 1. The standard atomic positions and isotopic atomic displacement parameters are listed in Table 2. The anisotropic displacement parameters and important bond lengths are listed in Tables 3 and 4, respectively. Further information on the structure refinements is available from: by quoting the Registry No. CCDC 989027.

2.5 Magnetic Measurements

Magnetic measurements on selected single crystals of $Yb_7Ni_4InGe_{12}$ were carried out on a Quantum Design MPMS-SQUID magnetometer. Temperature dependent magnetic data were collected for field cooled mode (FC) between 2 to 400 K in an applied field (H) of 1000 Oe. Magnetization data were also collected for $Yb_7Ni_4InGe_{12}$ at 2 K and 300 K with field sweeping from -60000 Oe to 60000 Oe.

2.6 X-ray Absorption Near-Edge Spectroscopy (XANES). XANES experiments were performed at the Sector 20 bending magnet beamline (PNC/XSD, 20-BM), of the Advanced Photon Source at the Argonne National Laboratory. Measurements at the Yb L_{III} edge were performed in the transmission mode using gas ionization chambers to monitor the incident and transmitted X-ray intensities. A third ionization chamber was used in conjunction with a copper foil to provide internal calibration for the alignment of the edge positions. Monochromatic X-rays was obtained using a Si (111) double crystal monochromator. The monochromator was calibrated by defining the inflection point (first derivative maxima) of Cu foil as 8980.5 eV. A Rh-coated X-ray mirror was utilized to suppress higher-order harmonics. XANES samples were prepared by mixing an appropriate amount of the finely ground $Yb_7Ni_4InGe_{12}$ with BN. The mixture was pressed to form a self-supporting pellet and the measurements were performed at 300 K and 18 K. Care was taken to suppress distortion in the data from thickness effects.

3. Results and Discussion

3.1 Reaction Chemistry

Metal flux technique plays a vital role in the development of new and complex intermetallic materials compared to conventional ceramic, arc melting and high frequency induction furnace heating methods. Among the wide range of metal fluxes available, indium

metal is highly attractive due to its low melting temperature (157 ^{0}C) and high boiling temperature (2072 ^{0}C). It has been widely used for the synthesis and crystal growth of indium-rich binary and ternary compounds and a few quaternary compounds as well. High-quality single crystals are generally required for the structure refinements for a new compound, which can be grown from a flux. The new compound $Yb_7Ni_4InGe_{12}$ was discovered in a reaction that was run in indium flux with the ratio of Yb:Ni:Ge:In as 4:2:5:35. In addition to $Yb_7Ni_4InGe_{12}$, single crystals of Yb_2InGe_2[73, 74] and $YbNiIn_2$[75] were also observed in small quantity. The amount of indium taken for the synthesis of these phases played a crucial role. While decreasing the amount of indium from 2.32 g to 1.99 g and then to 1.66 g, the compounds Yb_2InGe_2 and $YbNiIn_2$, respectively, were obtained as major products. Interestingly, in all these reactions indium act as reactive flux. In our earlier report, the composition 5:4:10:45 for Yb:Ni:Ge:In favored in the formation of $Yb_5Ni_4Ge_{10}$, however interestingly no inclusion of the In atom into structure occurred.[60] Our attempts to synthesize the similar composition to $Yb_7Ni_4InGe_{12}$ with other rare earth metals were not successful. We also could not prepare pure phase of $Yb_7Ni_4InGe_{12}$ using a high frequency induction heating method. The single crystals of $Yb_7Ni_4InGe_{12}$ are metallic silver in color and stable in air and no decomposition observed even after several months. The SEM images of typical single crystals of $Yb_7Ni_4InGe_{12}$ are shown in Figure 1.

3.2 Crystal chemistry

$Yb_7Ni_4InGe_{12}$ crystallizes in the tetragonal structure of the $Yb_7Co_4InGe_{12}$ type (space group $P4/m$). The crystal structure of $Yb_7Ni_4InGe_{12}$ is composed of a complex $[Ni_4InGe_{12}]$ polyanionic network with three different types of one-dimensional channels. These channels are constructed by five, six and eight membered rings propagated along the c-direction with

different types of ytterbium atoms embedded in them. These three different type channels are interconnected through edge and corner sharing form a three dimensional network. The crystal structure of $Yb_7Ni_4InGe_{12}$ is similar to the compounds crystallize in the $Sc_5Co_4Si_{10}$ type structure.[60, 76] The comparison between $Yb_5Ni_4Ge_{10}$ and $Yb_7Ni_4InGe_{12}$ structures shown in Figure 2 clearly suggest the atomic arrangements in both compounds are similar. Both compounds crystallize in the tetragonal system, but different space groups; $P4/m$ for $Yb_7Ni_4InGe_{12}$ and $P4/mbm$ for $Yb_5Ni_4Ge_{10}$. In $Yb_7Ni_4InGe_{12}$, the twofold rotation axis with centre of symmetry (2/m) and twofold screw axis (2_1) are absent compared to $Yb_5Ni_4Ge_{10}$.

In both structures, the widest channels in the structure are built from stacked alternating planar octagonal and square rings interconnected via Ni–Ge and Ge–Ge bonds, in which the octagons are defined by alternating four Ni and four Ge atoms, and the square rings are composed of four Ge atoms. In $Yb_5Ni_4Ge_{10}$, Yb1 atoms are sitting in the center of the octagonal rings, whereas in $Yb_7Ni_4InGe_{12}$, it is occupied by the Yb3 atom. The Ge-Ge distance in the square ring can be considered as a weak bonding interaction because of the large interatomic distance of 2.9162(3) Å and 2.973(4), respectively for $Yb_5Ni_4Ge_{10}$ and $Yb_7Ni_4InGe_{12}$. The eight membered rings are surrounded by four six membered rings and four five membered rings arranged opposite to each other. However the notable difference is in the distribution of pentagonal and hexagonal rings. As shown in Figure 3, in the quaternary compound, the four pentagons are shared through edges and one common In corner, while in $Yb_5Ni_4Ge_{10}$, they are separated by Ni-Ge and Ge-Ge bonds. This difference is reflected in the bond distance and bond angles as well. The bond distances and bond angles in both compounds are close except in five membered rings. In $Yb_7Ni_4InGe_{12}$ bond distance of Yb1-In in five membered channel is 3.3267(1) Å and bond angle of Ge1-In-Ge1 is 90^0 (marked in figure 2a)

and $Yb_5Ni_4Ge_{10}$ bond distance of Yb2-Ge1 in five membered ring is 2.8470(3) Å and bond angle of Ge1-Ni-Ge2 is 105^0 (marked in figure 2b). The hexagons in $Yb_7Ni_4InGe_{12}$ exist as individual unit with a separation of Ni-Ge bonds between them, whereas, in $Yb_5Ni_4Ge_{10}$, they exist as dimers with edge sharing. The hexagonal rings in $Yb_7Ni_4InGe_{12}$ are more distorted with bond angles in the range $113-129^0$ compared $115-121^0$ in the case of ternary compound clearly indicates a reduction of symmetry in the quaternary compound.

The average Yb-Ni bond distance in the $Yb_7Ni_4InGe_{12}$ crystal structure calculated as 3.151(1) Å, which is close to the atomic radii of Yb-Ni distance (3.124 Å) observed in Yb_2NiGe_6[59] and the calculated distance of 3.110 Å.[71, 72] The average distance obtained for Yb1-Ge and Yb2-Ge bonds are 2.989 Å and 2.953 Å, respectively, smaller than the calculated distances of Yb^{2+}-Ge (3.08 Å)[71, 72] and larger than Yb^{3+}-Ge (2.91 Å)[71, 72] suggest mixed or intermediate valency of Yb atoms in $Yb_7Ni_4InGe_{12}$.[36] A similar mixed valent behavior was noticed in the prototype compound $Yb_7Co_4InGe_{12}$. However, shorter Yb1-Ge and Yb2-Ge distances (2.904 Å and 2.953 Å) and larger Yb3-Ge distance (3.056 Å) suggest Yb1 and Yb2 are in the trivalent and Yb3 in the divalent oxidation states. Based on these bond analyses it can be speculated that Yb atoms in $Yb_7Ni_4InGe_{12}$ exist as divalent and trivalent valent states. Moreover our magnetism data, which will be discussed in the next section also support the mixed valence behavior. The overall Yb valency calculated by considering the quantitative atomic contribution taken from the Wyckoff sites as 72% trivalent Yb, which is close to the value of 80% obtained from the magnetic data. The slight increase of the oxidation state of Yb^{3+} observed in the magnetic data perhaps due to the impurity of Yb^{3+} oxide present in the sample. The average bond distance between Yb3 and Ge atoms is 3.173(1) Å, close to the Yb-Ge distance observed in $Yb_7Co_4InGe_{12}$ (3.16 Å) and the calculated value of 3.16 Å.[36]

The local coordination environments of ytterbium, germanium, nickel and indium atoms in the crystal structure of $Yb_7Ni_4InGe_{12}$ are compared in Figures 4 and 5 with the coordination environments of the atoms in $Yb_5Ni_4Ge_{10}$. Crystallographically there are three distinct Yb atoms present in both structures. While adopting standard atomic coordinates of the reported $Yb_5Ni_4Ge_{10}$ structure, the coordination sphere of Yb1, Yb2 and Yb3 in $Yb_7Ni_4InGe_{12}$ are closely related to the environment of Yb2, Yb3 and Yb1 in $Yb_5Ni_4Ge_{10}$. The notable difference is between Yb1 in $Yb_7Ni_4InGe_{12}$ and Yb2 in $Yb_5Ni_4Ge_{10}$, which is probably due to the presence of In the environment of Yb1 in $Yb_7Ni_4InGe_{12}$. This overall affects the distortion in the rings and aids the reduction in symmetry. Yb1 atom coordinates with eleven atoms with two pentagonal rings, made up of six Ge, two Ni and two indium atoms. These two pentagonal rings are connected by one Ge atom and host Yb1 atoms at the center. Yb3 atom is surrounded by twelve Ge atoms and four Ni atoms, whereas, the Yb1 atom, located at the hexagonal tunnel, is in contact with 10 Ge atoms and four Ni atoms. The coordination environment of Ni and Ge of both compounds are similar, see Figure 5.

3.4   Physical Properties

3.4.1   Magnetism of $Yb_7Ni_4InGe_{12}$

The temperature dependent molar magnetic susceptibility (χ_m) and inverse susceptibility ($1/\chi_m$) of $Yb_7Ni_4InGe_{12}$ at an applied field of 1000 Oe are shown in Figure 6. As it can be clearly seen, a continuous deviation from the linearity observed in the entire temperature range of measurement signaling non-Curie-Weiss (CW) type behavior. In order to explore the possibility of any large diamagnetic signal, the modified Curie-Weiss law was applied to the data. The constant susceptibility term, χ_0, was subtracted from the measured susceptibility data, and the inverse of the resultant ($\chi - \chi_0$) vs temperature also resulted in non-

linear behavior. This means that the system exhibits non-CW behavior and indicates neither a simple paramagnet nor complete magnetic ordering.

However, to get the magnetic moment, the high temperature inverse susceptibility data fitted with CW law, $\chi = C/(T-\theta_p)$,[77, 78] where C is the Curie-Weiss constant ($N_A\mu_{eff}^2/3K_bT$) and θ_p is the Weiss temperature. A fit to the curve above 200 K with an effective magnetic moment of 3.66 μ_B/Yb atom suggest mixed valent or intermediate valent nature of Yb atoms. The magnetic moment obtained above 200 K is close to value of the prototype compound $Yb_7Co_4InGe_{12}$.[36] The estimated experimental μ_{eff} values calculated above 200 K is about 80% of that expected for a free ion Yb^{3+} moment (4.56 μ_B/Yb). Magnetic susceptibility of $Yb_7Ni_4InGe_{12}$ shows no magnetic ordering down to 2 K but the susceptibility slightly increases at lower temperature with increasing field, which is normal for rare earth based intermetallics.[52, 60, 79] This deviation can be attributed to crystal field contributions, magnetic impurities and/or valence fluctuations. However, a detailed analysis such as inelastic neutron scattering and [170]Yb Mössbauer spectroscopy are need to be done to confirm these speculations, which are beyond the scope of this report.

The field dependence of the magnetization $M(H)$ for ground sample of $Yb_7Ni_4InGe_{12}$ was measured at 2 K and 300 K is shown in Figure 7. The data measured at 300 K exhibit linear behavior up to highest field of 60000 Oe and no show sign of saturation. The magnetization curve taken at 2 K shows a slight field dependent response up to ~ 30000 Oe, continues to rise slowly up to the highest obtainable field 60000 Oe without any hint of saturation.

3.4.2 XANES

XANES measurements were performed at the Yb L_{III}-edge, at ambient pressure and at two different temperatures (300 K and 18 K), to probe the Yb valence state in $Yb_7Ni_4InGe_{12}$. The intense absorption peak (white line resonance) of the spectrum (Figure 8) centered at ~8948 eV, which is attributed to trivalent Yb atoms.[80-83] The spectra also revealed the presence of a weaker feature (shoulder) at ~8940 eV, revealing clearly that some divalent Yb ions ($4f^{14}$) are also present.[80-83] From the XANES measurements, the compound $Yb_7Ni_4InGe_{12}$ can be classified as either as an intermediate valence compound with all three Yb atoms having a non-integer valence or heterogeneous mixed-valence compound, in which specific Yb atoms are either exactly 2+ or 3+. The relative amounts of the two electronic configurations were estimated by decomposing the normalized Yb XANES into a pair of arc-tangents (representing the edge step) and Lorentzian functions (representing the white line resonance).[36] Fitting of the data with the above technique resulted in ~ 73(5)% Yb^{3+} corresponds to an average Yb valence of ~ 2.73. This value is in reasonable agreement with magnetic measurements. The uncertainty in the absolute valence is ~5%, arising from correlations between parameters used to represent the edge-step and white line resonances and from systematic errors due to fitting-model dependence. In addition, careful inspection shows that the relative intensity of the features at ~ 8948 and 8940 eV varies weakly with temperature. This change in intensity suggests that the Yb^{3+} state is slightly more populated at 295 K.

4. Concluding Remarks

A new quaternary phase $Yb_7Ni_4InGe_{12}$ was obtained as rod shaped crystals from the active indium flux. Our attempts to synthesize the phase by conventional direct synthesis techniques have not been successful, which indicates that the metal flux technique is a vital

synthesis method to obtain novel compounds and necessary for stabilizing these compounds. The compound adopts the $Yb_7Co_4InGe_{12}$ structure type. The crystal structures of $Yb_7Ni_4InGe_{12}$ and $Yb_5Ni_4Ge_{10}$ are closely related to each other. The magnetic susceptibility and XANES measurements on $Yb_7Ni_4InGe_{12}$ suggest mixed/intermediate valent behavior for the ytterbium atoms, and point to potentially interesting electronic and magnetic physical properties.

Supporting information available: Crystallographic information files (CIF). This material is available free of charge via the Internet. The CCDC reference number for $Yb_7Ni_4InGe_{12}$ is 989027.

References

1.   M. F. Hundley, J. L. Sarrao, J. D. Thompson, R. Movshovich, M. Jaime, C. Petrovic and a. Z. Fisk, *Phys. Rev. B*, 2001, **65**, 024401.

2.   R. T. Macaluso, J. L. Sarrao, N. O. Moreno, P. G. Pagliuso, J. D. Thompson, F. R. Fronczek, M. F. Hundley, A. Malinowski and J. Y. Chan, *Chem. Mater.*, 2003, **15**, 1394-1398.

3.   J. R. Salvador, D. Bilc, J. R. Gour, S. D. Mahanti and M. G. Kanatzidis, *Inorg. Chem.*, 2005, **44**, 8670-86794.

4.   U. Subbarao and S. C. Peter, *J. Chem. Sci.*, 2013, **125**, 1315-1323.

5.   S. Sarkar and S. C. Peter, *Inorg. Chem.*, 2013, **52**, 9741-9748.

6.   U. Subbarao, A. Sebastian, S. Rayaprol, C. S. Yadav, A. Svane, G. Vaitheeswaran and S. C. Peter, *Cryst Growth Des*, 2013, **13**, 352-359.

7.   S. Sarkar, M. J. Gutmann and S. C. Peter, *Cryst. Growth Des.*, 2013, **13**, 4285-4294.

8.   S. Sarkar, M. J. Gutmann and S. C. Peter, *Crystengcomm*, 2013, **15**, 8006-8013.

9.   S. C. Peter, S. Sarkar and M. G. Kanatzidis, *Inorg Chem*, 2012, **51**, 10793-10799.

10.   S. Sarkar and S. C. Peter, *J Chem Sci*, 2012, **124**, 1385-1390.

11.   S. C. Peter, C. D. Malliakas, H. Nakotte, K. Kothapilli, S. Rayaprol, A. J. Schultz and M. G. Kanatzidis, *J. Solid State Chem.*, 2012, **187**, 200-207.

12.   X. Z. Chen, S. Sportouch, B. Sieve, P. Brazis, C. R. Kannewurf, J. A. Cowen, R. Patschke and M. G. Kanatzidis, *Chem. Mater.*, 1998, **10**, 3202-3211.

13.   U. Subbarao, S. Sarkar, V. K. Gudelli, V. Kanchana, G. Vaitheeswaran and S. C. Peter, *Inorg. Chem.*, 2013, **52**, 13631-13638.

14.   S. M. Disseler, J. N. Svensson, S. C. Peter, C. P. Byers, C. Baines, A. Amato, S. R. Giblin, P. Carretta and M. J. Graf, *Phys. Rev. B*, 2011, **84**, 174429-174437.

15.   S. C. Peter, M. Chondroudi, C. D. Malliakas, M. Balasubramanian and M. G. Kanatzidis, *J Am Chem Soc*, 2011, **133**, 13840-13843.

16.   S. C. Peter, U. Subbarao, S. Sarkar, G. Vaitheeswaran, A. Svane and M. G. Kanatzidis, *J. Alloys Compd.*, 2014, **589**, 405-411.

17.   S. C. Peter and M. G. Kanatzidis, *Z Anorg Allg Chem*, 2012, **638**, 287-293.

18.   X. Z. Chen, P. Larson, S. Sportouch, P. Brazis, S. D. Mahanti, C. R. Kannewurf and M. G. Kanatzidis, *Chem. Mater.*, 1999, **11**, 75-83.

19.   B. Sieve, X. Z. Chen, R. Henning, P. Brazis, C. R. Kannewurf, J. A. Cowen, A. J. Schultz and M. G. Kanatzidis, *J Am Chem Soc*, 2001, **123**, 7040-7047.

20.   M. A. Zhuravleva, R. J. Pcionek, X. P. Wang, A. J. Schultz and M. G. Kanatzidis, *Inorg. Chem.*, 2003, **42**, 6412-6424.

21.   M. A. Zhuravleva, M. Evain, V. Petricek and M. G. Kanatzidis, *J. Am. Chem. Soc*, 2007, **129**, 3082-3083.

22.   X. Z. Chen, P. Small, S. Sportouch, M. Zhuravleva, P. Brazis, C. R. Kannewurf and M. G. Kanatzidis, *Chem. Mater.*, 2000, **12**, 2520-2522.

23.   S. E. Latturner, D. Bilc, S. D. Mahanti and M. G. Kanatzidis, *Inorg. Chem.*, 2003, **42**, 7959-7966.

24.   X. U. Wu, S. E. Latturner and M. G. Kanatzidis, *Inorg. Chem.*, 2006, **45**, 5358-5366.

25.   S. E. Latturner, D. Bilc, S. D. Mahanti and M. G. Kanatzidis, *Chem. Mater.*, 2002, **14**, 1695-1705.

26.   J. R. Salvador, K. Hoang, S. D. Mahanti and M. G. Kanatzidis, *Inorg. Chem.*, 2007, **46**, 6933.

27.   C. P. Sebastian, C. D. Malliakas, M. Chondroudi, I. Schellenberg, S. Rayaprol, R. D. Hoffmann, R. Pottgen and M. G. Kanatzidis, *Inorg Chem*, 2010, **49**, 9574-9580.

28.   J. R. Salvador, J. R. Gour, D. Bilc, S. D. Mahanti and M. G. Kanatzidis, *Inorg. Chem.*, 2004, **43**, 1403-1410.

29.   J. R. Salvador, C. Malliakas, J. R. Gour and M. G. Kanatzidis, *Chem Mater*, 2005, **17**, 1636-1645.

30.   M. S. Bailey, M. A. McCuire and a. F. J. DiSalvo, *J. Solid Sate Chem.*, 2005, **178**, 3494-3499.

31.   W. Klunter and W. Jung, *J. Solid Sate Chem.*, 2006, **179**, 2880-2888.

32.   V. I. Zaremba, V. P. Dubenskiy, U. C. Rodewald, B. Heying and R. Pöttgen, *J. Solid State Chem.*, 2006, **179**, 891-897.

33.   M. Lukachuk, Y. V. Galadzhun, R. I. Zaremba, M. V. Dzevenko, Y. M. Kalychak, V. I. Zaremba, U. C. Rodewald and R. Pöttgen, *J. Solid State Chem.*, 2005, **178**, 2724-2733.

34. R. T. Macaluso, J. L. Sarrao, P. G. Pagliuso, N. O. Moreno, R. G. Goodrich, D. A. Browne, F. R. Fronczek and J. Y. Chan, *J. Solid Sate Chem.*, 2002, **166**, 245-250.

35. J. R. Salvador and M. G. Kanatzidis, *Inorg. Chem.*, 2006, **45**, 7091-7099.

36. M. Chondroudi, M. Balasubramanian, U. Welp, W. K. Kwok and M. G. Kanatzidis, *Chem. Mater.*, 2007, **19**, 4769-4775.

37. M. G. Kanatzidis, R. Pöttgen and W. Jeitschko, *Angew. Chem. Int. Ed.*, 2005, **44**, 6996-7023.

38. U. Subbarao, M. J. Gutmann and S. C. Peter, *Inorg. Chem.*, 2013, **52**, 2219-2227.

39. C. P. Sebastian, J. Salvador, J. B. Martin and M. G. Kanatzidis, *Inorg Chem*, 2010, **49**, 10468-10474.

40. C. P. Sebastian and M. G. Kanatzidis, *J. Solid State Chem.*, 2010, **183**, 2077-2081.

41. Y. Matsumoto, S. Nakatsuji, K. Kuga, Y. Karaki, N. Horie, Y. Shimura, T. Sakakibara, A. H. Nevidomskyy and P. Coleman, *Science*, 2011, **331**, 316-319.

42. S. Ernst, S. Kirchner, C. Krellner, C. Geibel, G. Zwicknagl, F. Steglich and S. Wirth, *Nature*, 2011, **474**, 362-366.

43. O. Stockert, J. Arndt, E. Faulhaber, C. Geibel, H. S. Jeevan, S. Kirchner, M. Loewenhaupt, K. Schmalzl, W. Schmidt, Q. Si and F. Steglich, *Nat. Phys.*, 2011, **7**, 119-124.

44. B. Kindler, D. Finsterbusch, R. Graf, F. Ritter, W. Assmus and B. Luthi, *Phys. Rev. B*, 1994, **50**, 704-707.

45. E. Bauer, *Adv. Phys.*, 1991, **40**, 417-534.

46. L. S. Hausermannberg and R. N. Shelton, *Phys. Rev. B*, 1987, **35**, 6659-6664.

47. H. F. Braun and C. U. Segre, *Solid State Commun.*, 1980, **35**, 735-738.

48. J. M. Lawrence, P. S. Riseborough and R. D. Park, *Rep. Prog. Phys.*, 1981, **44**, 1-84.

49. Z. Fisk, D. W. Hess, C. J. Pethick, D. Pines, J. L. Smith, J. D. Thompson and J. O. Willis, *Science*, 1988, **239**, 33-42.

50. U. Subbarao and S. C. Peter, *Cryst. Growth Des.*, 2013, **13**, 953-959.

51. U. Subbarao and S. C. Peter, *Inorg Chem*, 2012, **51**, 6326-6332.

52. M. Chondroudi, S. C. Peter, C. D. Malliakas, M. Balasubramanian, Q. A. Li and M. G. Kanatzidis, *Inorg Chem*, 2011, **50**, 1184-1193.

53. S. C. Peter, S. M. Disseler, J. N. Svensson, P. Carretta and M. J. Graf, *J. Alloys Compd.*, 2012, **516**, 126-133.

54. S. C. Peter, J. Salvador, J. B. Martin and M. G. Kanatzidis, *Inorg. Chem.*, 2010, **49**, 10468-10474.

55. S. C. Peter and M. G. Kanatzidis, *J Solid State Chem*, 2010, **183**, 2077-2081.

56. R. B. Dzyanyi, O. I. Bodak and V. B. Pavlyuk, *Russ. Metall.*, 1995, 133-135.

57. Y. K. Gorelenko, P. K. Starodub, V. A. Bruskov, R. V. Skolozdra, V. I. Yarovets, O. I. Bodak and V. K. Pecharskii, *Ukr. Fiz. Zh.*, 1984, **29**, 867-871.

58. W. Rieger and E. Parthé, *Monatsh. Chem.*, 1969, **100**, 444-454.

59. K. Shigetoh, D. Hirata, M. A. Avila and T. Takabatake, *J. Alloys Compd.*, 2005, **403**, 15-18.

60. S. C. Peter, S. Rayaprol, M. C. Francisco and M. G. Kanatzidis, *Eur J Inorg Chem*, 2011, 3963-3968.

61. D. Rossi, R. Ferro, V. Contardi and R. Marazza, *Z. Metallkd.*, 1977, **68**, 493-497.

62. E. M. Benbow and S. E. Latturner, *J. Solid State Chem.*, 2006, **179**, 3989-3996.

63. C. Lefevre, G. Venturini and B. Malaman, *J. Alloys Compd.*, 2003, **358**, 29-35.

64. R. A. Gordon, Y. Ijiri, C. M. Spencer and F. J. Disalvo, *J. Alloys Compd.*, 1995, **224**, 101-107.

65. K. M. Poduska, F. J. DiSalvo and V. Petricek, *J. Alloys Compd.*, 2000, **308**, 64-70.

66. D. Dominyuk, V. I. Zaremba and R. Pöttgen, *Z. Naturforsch.*, 2011, **66b**, 433-436.

67. R. Lahiouel, J. Pierre, E. Siaud and A. P. Murani, *J. Magn. Magn. Mater.*, 1987, **63-4**, 104-106.

68. SAINT, Bruker AXS Inc., Madison, Wisconsin, USA, 6.02 edn., 2000.

69. G. M. Sheldrick, ed., SADABS, Göttingen, Germany, 1997.

70. S. A. Acta Crystallogr., *Acta Crystallogr., Sect. A*, 2008, **64**, 112-122.

71. F. H. Allen, O. Kennard, D. G. Watson, L. Brammer, A. G. Orpen and R. Taylor, *J. Chem. Soc.*, 1987, **2**, S1–S19.

72. R. T. Sanderson, *JACS*, 1983, **105**, 2259–2261.

73. P. H. Tobash, D. Lins, S. Bobev, A. Lima, M. F. Hundley, J. D. Thompson and J. L. Sarrao, *Chem. Mater.*, 2005, **17**, 5567-5573.

74. V. I. Zaremba, Y. B. Tyvanchuk and J. Stepien-Damm, *Z. Krist. New Cryst. St.*, 1997, **212**, 291-291.

75. V. I. Zaremba, I. R. Muts, U. C. Rodewald, V. Hlukhyy and R. Pöttgen, *Z. Anorg. Allg. Chem.*, 2004, **630**, 1903-1907.

76. H. F. Braun, K. Yvon and R. M. Braun, *Acta Crystallogr. B*, 1980, **36**, 2397-2399.

77. J. S. Smart, *Effective Field Theories of Magnetism*, Philadelphia, Pennsylvania, 1966.

78. C. Kittel, *Introduction to Solid State Physics* John Wiley & Sons, Hoboken, NJ, 1996.

79. S. C. Peter, H. Eckert, C. Fehse, J. P. Wright, J. P. Attfield, D. Johrendt, S. Rayaprol, R. D. Hoffmann and R. Pöttgen, *J. Solid State Chem.*, 2006, **179**, 2376-2385.

80. M. Chondroudi, S. C. Peter, C. D. Malliakas, M. Balasubramanian, Q. A. Li and M. G. Kanatzidis, *Inorg. Chem.*, 2011, **50**, 1184-1193.

81. C. N. R. Rao, D. D. Sarma, P. R. Sarode, E. V. Sampathkumaran, L. C. Gupta and R. Vijayaraghavan, *Chem. Phys. Lett.*, 1980, **76**, 413-415.

82. T. K. Hatwar, R. M. Nayak, B. D. Padalia, M. N. Ghatikar, E. V. Sampathkumaran, L. C. Gupta and R. Vijayaraghavan, *Solid State Commun.*, 1980, **34**, 617-620.

83. L. Moreschini, C. Dallera, J. J. Joyce, J. L. Sarrao, E. D. Bauer, V. Fritsch, S. Bobev, E. Carpene, S. Huotari, G. Vanko, G. Monaco, P. Lacovig, G. Panaccione, A. Fondacaro, G. Paolicelli, P. Torelli and M. Grioni, *Phys. Rev. B*, 2007, **75**.

Tables:

Table 1. Crystal data and structure refinement for $Yb_7Ni_4InGe_{12}$ at 296(2) K.

Empirical formula	$Yb_7Ni_4InGe_{12}$
Formula weight	2432.02
Wavelength	0.71073 Å
Crystal system	Tetragonal
Space group	*P4/m*
Unit cell dimensions	$a = b = 10.291(2)$ Å $c = 4.1460(8)$ Å
Volume	439.1(2) $Å^3$
Z	1
Density (calculated)	9.2 g/cm^3
Absorption coefficient	62.44 mm^{-1}
F(000)	1034.4
Crystal size	0.05 x 0.05 x 0.10 mm^3
θ range for data collection	1.98 to 25.00°
Index ranges	$-12 <= h <= 11$ $-11 <= k <= 12$ $-4 <= l <= 4$
Reflections collected	3545
Independent reflections	387 [$R_{int} = 0.0782$]
Completeness to $\theta = 30.55°$	100%
Refinement method	Full-matrix least-squares on F^2
Data / restraints / parameters	387/ 0 / 40
Goodness-of-fit	1.170
Final *R* indices [$>2\sigma(I)$]	$R_{obs} = 0.042$, $wR_{obs} = 0.108$
Extinction coefficient	0.010792(1)
Largest diff. peak and hole	3.184 and -4.485 $e \cdot Å^{-3}$

$R = \Sigma||F_o|-|F_c|| / \Sigma|F_o|$, $wR = \{\Sigma[w(|F_o|^2 - |F_c|^2)^2] / \Sigma[w(|F_o|^4)]\}^{1/2}$ and calc $w=1/[\sigma^2(Fo^2)+(0.0359P)^2+6.1794P]$ where $P=(Fo^2+2Fc^2)/3$

Table 2. Atomic coordinates (x10^4) and equivalent isotropic displacement parameters (Å^{2}x10^3) for Yb$_7$Ni$_4$InGe$_{12}$ at 296(2) K with estimated standard deviations in parentheses.

Label	Wyckoff site	x	y	z	Occupancy	U_{eq}*
Yb1	4k	3273(1)	3256(1)	5000	1	6(1)
Yb2	1a	0	0	0	1	6(1)
Yb3	2f	0	5000	5000	1	8(1)
Ni	4j	1194(3)	2800(3)	0	1	6(1)
In	1c	5000	5000	0	1	9(1)
Ge1	4j	2180(2)	4903(2)	0	1	6(1)
Ge2	4j	2878(3)	1134(3)	0	1	20(1)
Ge3	4k	673(3)	1929(3)	5000	1	18(1)

Table 3. Anisotropic displacement parameters (Å^{2}x10^3) for Yb$_7$Ni$_4$InGe$_{12}$ at 296(2) K with estimated standard deviations in parentheses.

Label	U_{11}	U_{22}	U_{33}	U_{12}	U_{13}	U_{23}
Yb1	5(1)	5(1)	9(1)	2(1)	0	0
Yb2	5(1)	5(1)	9(1)	0	0	0
Yb3	4(1)	8(1)	11(1)	0	0	0
Ge1	4(1)	3(1)	12(1)	0	0	0
Ni	5(1)	5(1)	10(2)	-1(1)	0	0
In	7(1)	7(1)	15(2)	0	0	0
Ge2	13(1)	11(1)	36(2)	1(1)	0	0
Ge3	30(1)	14(2)	9(2)	-15(1)	0	0

The anisotropic displacement factor exponent takes the form: $-2\pi^2[h^2a^{*2}U_{11} + ... + 2hka^*b^*U_{12}]$.

Table 4. Selected bond lengths [Å] for $Yb_7Ni_4InGe_{12}$ at 296(2) K with estimated standard deviations in parentheses.

Label	Distances	Label	Distances
Yb1—Ge1	2.9041(19)	Yb3—Ge1	3.056(18)
Yb1—Ge1	3.008(19)	Yb3—Ge2	3.229(2)
Yb1—Ge2	3.039(2)	Yb3—Ge3	3.235(3)
Yb1—Ge3	3.005(3)	Yb3—Ni	3.306(2)
Yb1—Ni	3.017(2)	Ge1—Ni	2.390(4)
Yb1—In	3.267(8)	Ge1—In	2.904(2)
Yb1—Yb1	3.5709(15)	Ge2—Ni	2.396(4)
Yb2—Ge3	2.953(2)	Ge2—Ge1	2.525(4)
Yb2—Ni	3.132(3)	Ge3—Ni	2.3210(19)

Figures:
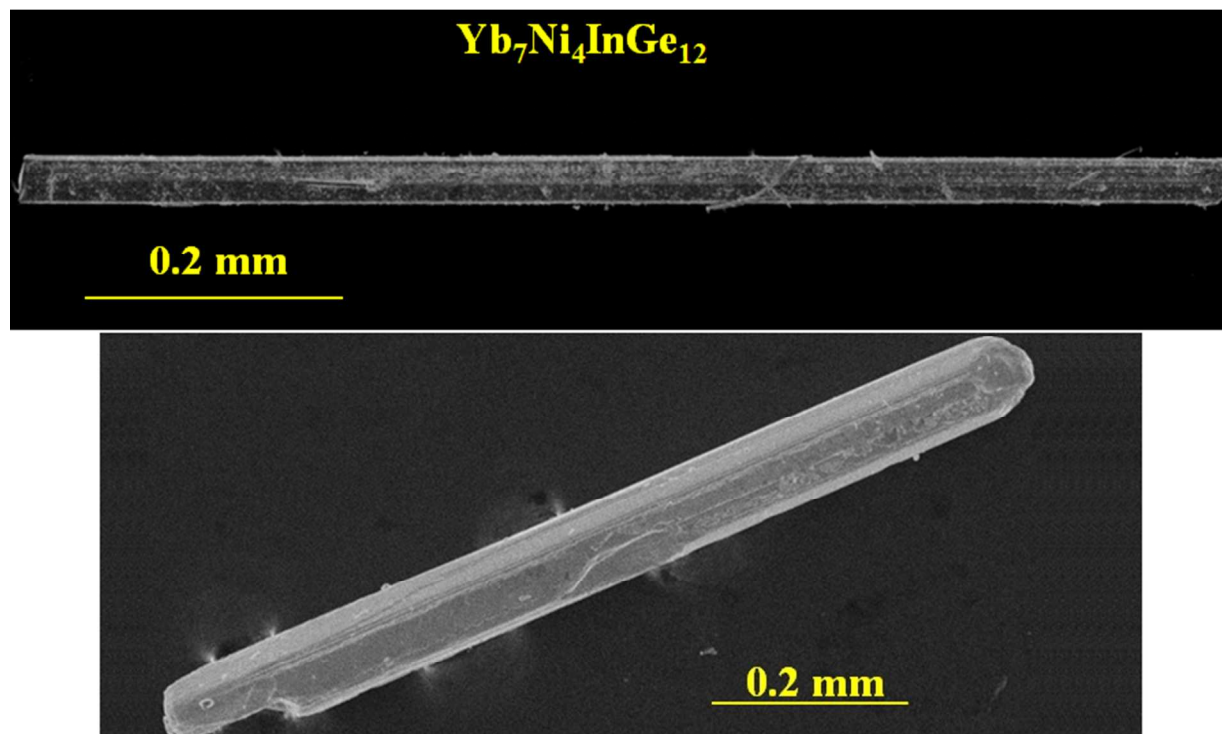
Figure 1. SEM images of the typical single crystals of $Yb_7Ni_4InGe_{12}$ grown from indium flux.
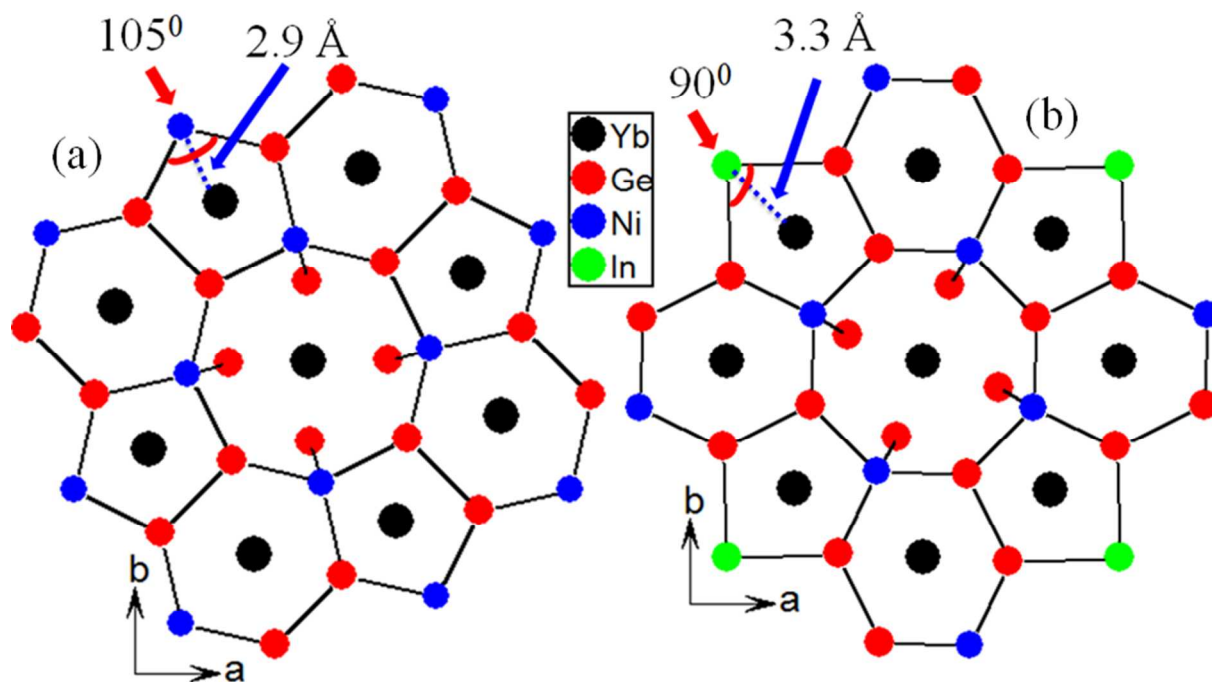
Figure 2. Crystal structure comparison of (a) $Yb_5Ni_4Ge_{10}$ and (b) $Yb_7Ni_4InGe_{12}$ is viewed in the *ab*-plane. Both structures consist of eight-membered ring with surrounding five and six membered rings.
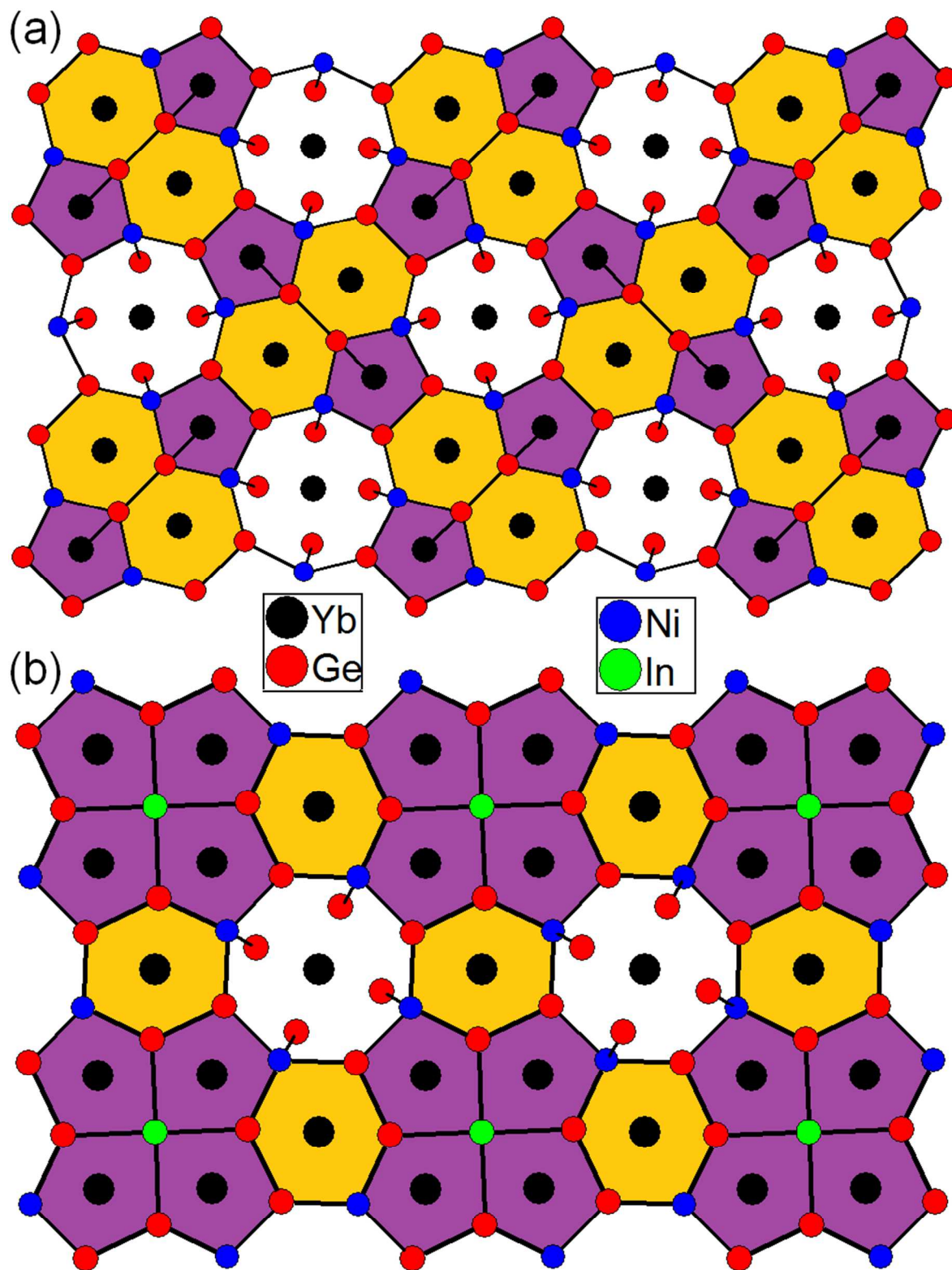
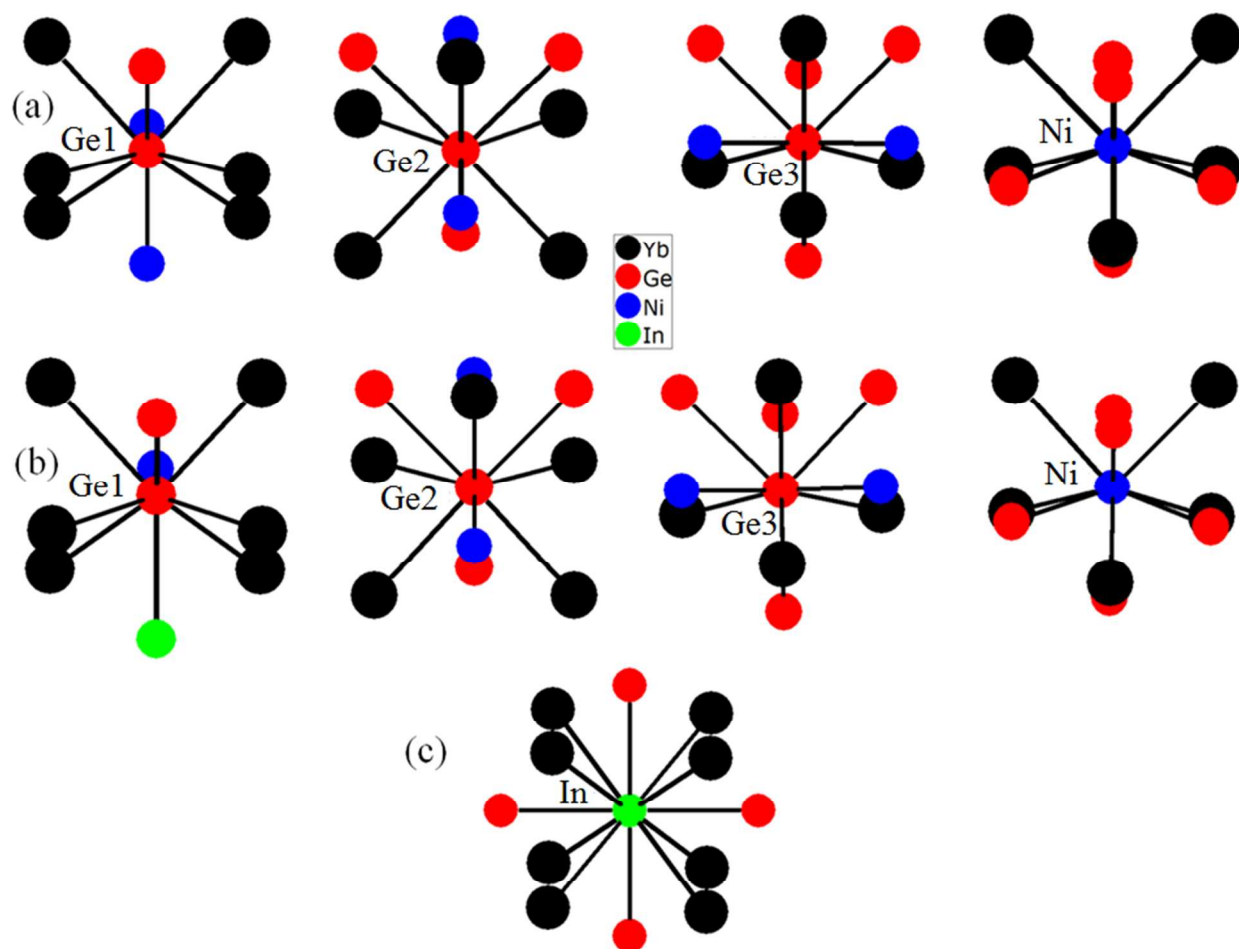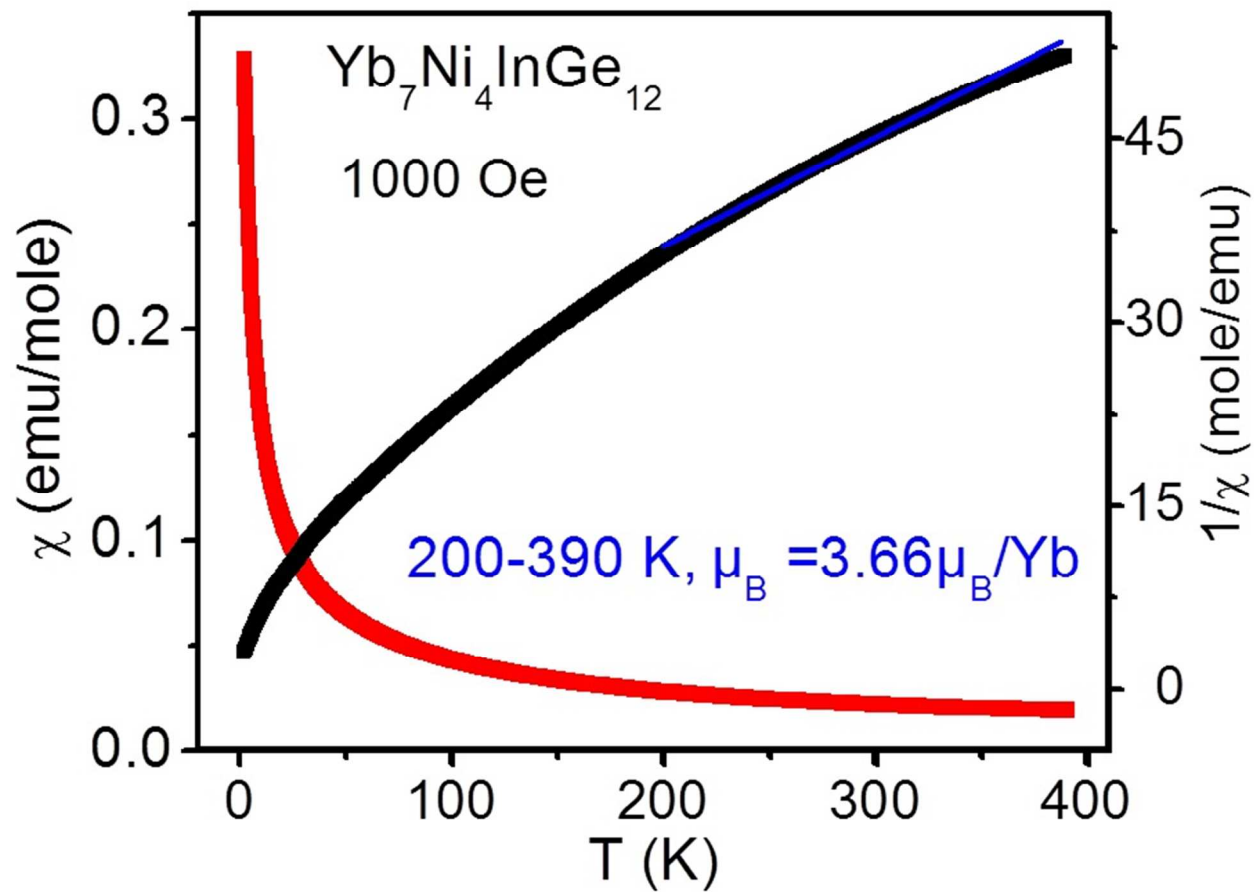**Figure 3.** Comparison of the crystal structures of (a) $Yb_5Ni_4Ge_{10}$ and (b) $Yb_7Ni_4InGe_{12}$ viewed along the c -axis.
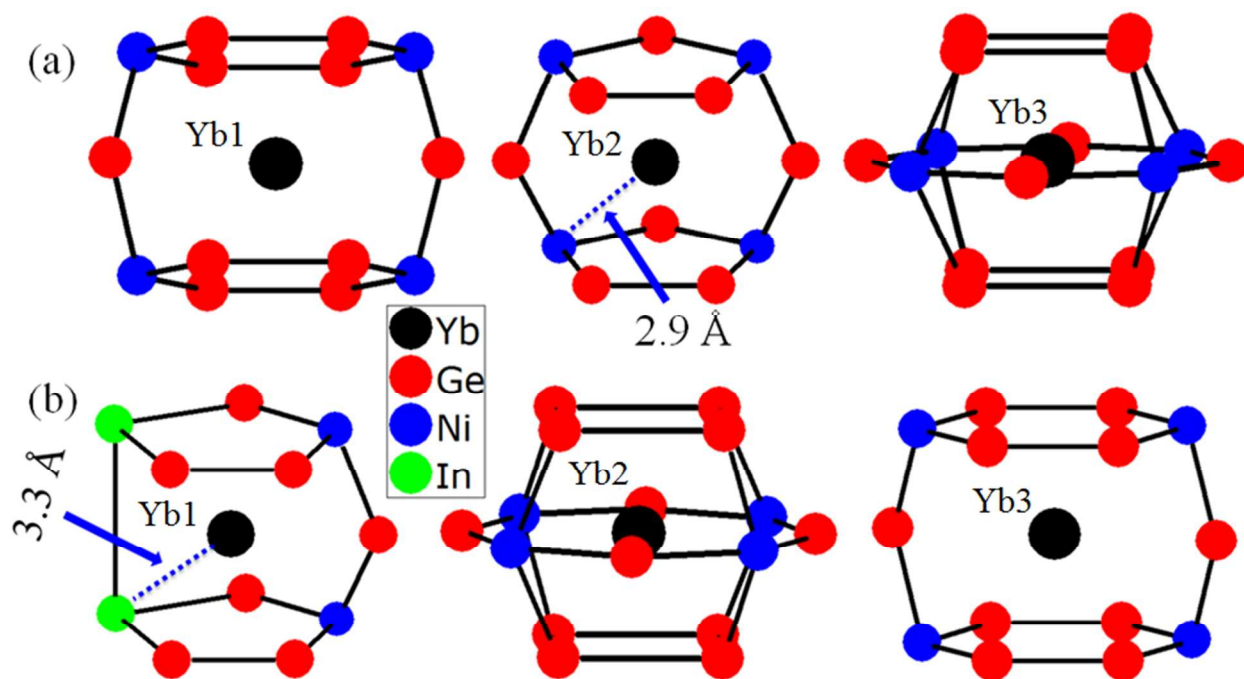
Figure 4. The coordination sphere of all Yb atoms in in (a) $Yb_5Ni_4Ge_{10}$ and (b) $Yb_7Ni_4InGe_{12}$.

Figure 5. The coordination sphere of Ge and Ni and In atoms in (a) $Yb_5Ni_4Ge_{10}$ and (b) $Yb_7Ni_4InGe_{12}$ are presented. (c) the coordination environment of In atom in $Yb_7Ni_4InGe_{12}$.

Figure 6. Temperature dependence of the magnetic susceptibility (χ_m) and inverse susceptibility ($1/\chi_m$) for a polycrystalline sample of $Yb_7Ni_4InGe_{12}$ measured at 1000 Oe applied field.
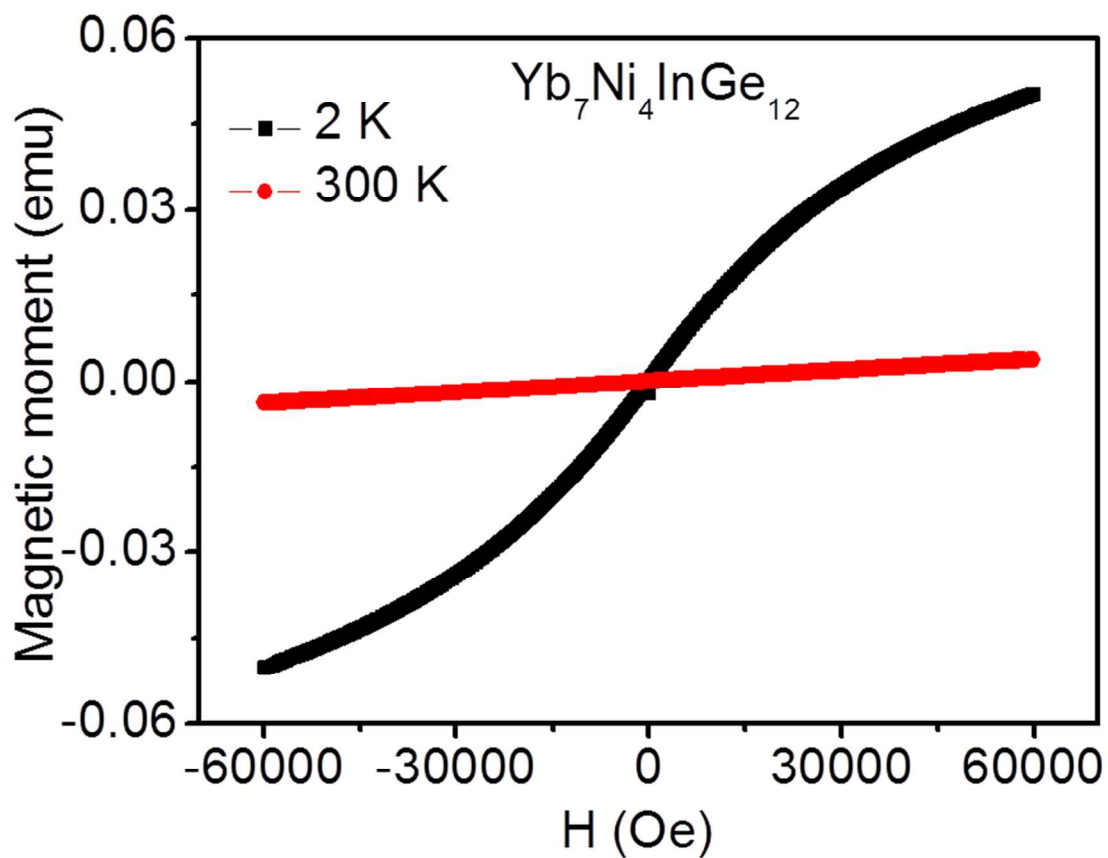
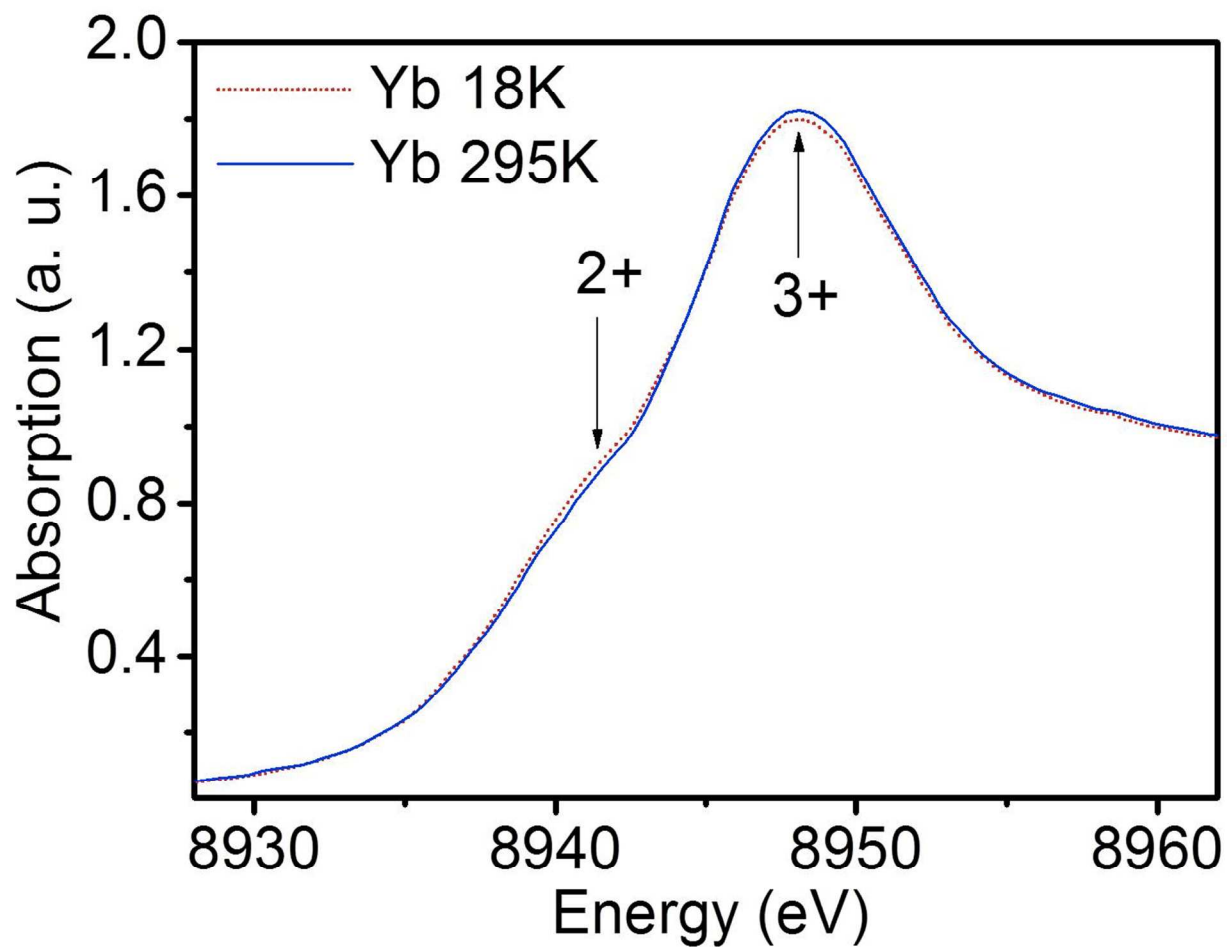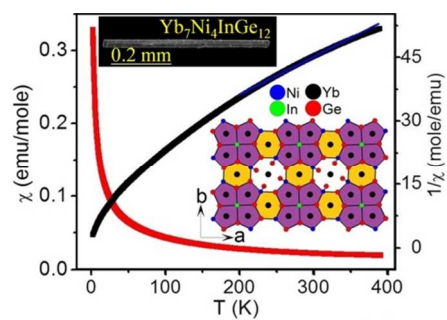**Figure 7.** Magnetization as a function of applied magnetic field at 2 K and 300 K for $Yb_7Ni_4InGe_{12}$.

Figure 8. Yb L$_{III}$ absorption edge spectra taken from a polycrystalline samples of Yb$_7$Ni$_4$InGe$_{12}$ at 300 K and 18 K.

For The Table of Contents Only

Graphical Abstract

$Yb_7Ni_4InGe_{12}$ is a new compound crystallzing from indium metal flux. Magnetic susceptibility and XANES data suggest mixed valent Yb atoms.